INDIAN JOURNAL OF SCIENCE AND TECHNOLOGY

RESEARCH ARTICLE

Lung Tumor Classification using Hybrid Deep Learning and Segmentation by Fuzzy C Means

T S Chandrakantha[1]*, **Basavaraj N Jagadale**[1], **Omar Abdullah Murshed Farhan Alnaggar**[1]

1 Department of PG Studies and Research in Electronics, Kuvempu University Jnana Sahyadri, Shankaraghatta, Shimoga, 577451, Karnataka, India

OPEN ACCESS

Received: 03-11-2023

Accepted: 10-12-2023

Published: 05-01-2024

Citation: Chandrakantha TS, Jagadale BN, Alnaggar OAMF (2024) Lung Tumor Classification using Hybrid Deep Learning and Segmentation by Fuzzy C Means. Indian Journal of Science and Technology 17(1): 70-79. https://doi.org/10.17485/IJST/v17i1.2124

* **Corresponding author**.

chandrabeluved@gmail.com

Funding: None

Competing Interests: None

Published By Indian Society for Education and Environment (iSee)

ISSN
Print: 0974-6846
Electronic: 0974-5645

Abstract

Objectives: This study aims to employ a hybrid Deep Learning (DL) technique for automating tumor detection and classification in lung scans. **Methods:** The methodology involves three key stages: data preparation, segmentation using Fuzzy C Means (FCM), and classification using a hybrid DL model. The image dataset is sourced from the benchmark Lung Tumor (LT) data, and for segmentation, the FCM approach is applied. The hybrid DL model is created by combining a Pulse Coupled Neural Network (PCNN) and a Convolutional Neural Network (CNN). The study utilizes a dataset of 300 individuals from the NSCLC-Radiomics database. The validation process employs DICE and sensitivity for segmentation, while the hybrid model's confusion matrix elements contribute to performance validation. FCM and the hybrid model are employed for processing, segmenting, and classifying the images. Evaluation metrics such as Dice similarity and Sensitivity gauge the success of the segmentation method by measuring the intersection between ground truths and predictions. After segmentation evaluation, the classification process is executed, employing accuracy and loss in the training phase and metrics like accuracy and F1-score in the testing phase for model validation. **Findings:** The proposed approach achieves an accuracy of 97.43% and an F1-score of 98.28%. These results demonstrate the effectiveness of the suggested approach in accurately classifying and segmenting lung tumors. **Novelty:** The primary contribution of the research is a hybrid DL model based on PCCN+CCN. This ultimately raises the quality of the model, and these are carried out using real-time public medical images, demonstrating the model's originality.

Keywords: Lung; Tumor; Segmentation; Classification; Hybrid model

1 Introduction

Lung cancer persists as a major global health challenge, contributing significantly to the annual toll of fatalities worldwide. Early detection and precise segmentation of lung tumors play a pivotal role in enhancing patient outcomes and treatment efficacy.

Medical imaging modalities, such as computed tomography (CT) scans, have been extensively employed for lung tumor segmentation and classification. Traditional methods, like Fuzzy C Means (FCM), have been utilized for delineating lung tumors from CT images. FCM, a clustering algorithm, assigns membership values to each voxel based on its similarity to different tissue classes. Despite showing promising results, FCM may encounter challenges in accurately capturing the complex shapes and varying intensity patterns of lung tumors. In recent times, deep learning methods have shown efficacy as valuable tools in medical image segmentation. Convolutional Neural Networks (CNNs) particularly stand out for their outstanding performance across various segmentation tasks. [1]. By leveraging substantial amounts of annotated data, CNNs can learn intricate spatial and contextual features, facilitating accurate and efficient tumor segmentation.

To refine the segmentation and classification of lung tumors, hybrid approaches integrating traditional algorithms with deep learning techniques have been suggested. These methodologies seek to leverage the respective strengths of both approaches while addressing their individual limitations. By integrating the fuzzy clustering capabilities of FCM with the feature learning capabilities of CNNs, more robust and accurate lung tumor segmentation and classification can be achieved. The suggested task seeks to examine and assess the impact of a hybrid technique integrating deep learning with fuzzy C Means for segmenting and classifying lung tumors. By harnessing the complementary attributes of these methodologies, the study seeks to enhance the precision, efficiency, and dependability of lung tumor detection and classification.

The detection of Lung Tumors (LT) today is conducted using CT scan images and a computerized evaluation of Computer-Aided Diagnosis (CAD) technology. Various CAD systems, developed by different researchers based on deep learning (DL) algorithms, automatically extract crucial features from CT scan images. However, many parameters must be hand-crafted to determine ideal performance, making it challenging to replicate the superior results obtained using these techniques [2]. The challenges of detecting Lung Tumors (LT) underscore the critical need for rapid and precise assessment. Highlighting the labor-intensive and error-prone aspects of pathologist reviews, the study explores the prospect of leveraging Artificial Intelligence (AI) techniques, including machine learning (ML) and deep learning (DL), for the identification of lung tumors (LT) [3].

One of the major limitations of previous CAD systems is the difficulty in accurately segmenting nodules from the lobes' region due to the often-similar intensity levels in the image. Additionally, classification accuracy is compromised due to the use of numerous noisy and fewer features. In this article, we propose a novel approach using FMC for accurate nodules segmentation and a hybrid PCNN with a CNN to improve overall classification accuracy. The major contributions of our approach are as the following:

- Our integration model of PCNN and CNN enhances the technique of feature extraction by capturing hidden features.
- PCNN and CNN collectively improve classification accuracy.
- Compared to other models, our approach yields considerably better outcomes.

The upcoming sections of this article follow this structure: Section 2 explores related work, Section 3 presents the proposed methodology, Section 4 elaborates on the results and discussion, and, bringing the article to a close, Section 5 provides the conclusion.

2 Related Works

Nazir, I. et al. [4] suggested an Adaptive global thresholding method for lung segmentation, the CT image histogram is used to choose the threshold. Then, Laplacian pyramids are employed for picture decomposition and reconstruction after segmentation and for image fusion adaptive sparse representation is used. Transfer learning was implemented by Nishio, M. et al. [5] and pretrained on the artificial LUNA16 dataset, which was developed using a 3D graph cut and a generative adversarial network. U-net built the pretrained segmentation model, which demonstrated a 0.09 dice score better than un-transfer learning models. Paing, M. P. et al. [6] introduced a CAD approach based on locational features and double-staged classifications to detect and stage lung cancer from CT images. Initially, gray-level thresholding was used for tumor segmentation. Then, the tumors that are detected are identified through the extraction of locational features. Finally, CAD utilized a double-staged classification to obtain accurate and robust predictions: 1) for tumor detection and 2) for staging. Various classifiers such as DT, KNN, SVM, ET, and BPNN are used in both classification stages to test the best classification performance. It has been found that the highest values of average accuracy and staging are 92.8% and 90.6% achieved with the BPNN classifier. For classifying lung cancer staging, Fathalla, K. M. et al. [7] developed a multistage neuro-based computational approach on 3D-CT volumes. The issue of selecting discriminatory CT slices to create 3D volumes is handled by DETECT-LC. This is accomplished using k-means clustering and Haralick radiomics. ALT-CNN-DENSE Net is developed to discern between different stages and pathologies. In the realm of phenotyping, DETECT-LC attains a minimum accuracy of 0.92. Neal Joshua, E. S. et al. [8] utilized an enhanced 3D AlexNet with a lightweight architecture to classify lung nodules in CT images from the LUNA 16 database, achieving an accuracy of 97.17%. Chaunzwa, T. L. et al. [9] compared the performance of a fully connected VGG16 CNN classifier with conventional ML classifiers. The distinction between ADC and SCC was made using the classification models. The 4096 and 512 feature vectors produced by the VGG16 architecture were used by the conventional classifiers. The deep-radiomics method, which extracts a 4096 features vector from the final fully linked layer, resulted in the best performance. Attributes were chosen using principal component analysis and LASSO. KNN (k = 5) was used for classification. Marentakis et al.[10] compared KNN and SVM radiomics classifiers, various CNN architectures, and a combinatorial approach (CNN + LSTM + radiomics). LSTM+Inception achieved the highest accuracy and AuC. Khodabakhshi et al.[11] introduced a high-dimensional CT radiomics signature for NSCLC classification. Wavelet decomposition and LOG filtering of the images resulted in the generation of a collection of 1433 radiomics features. To categorise histological subtypes, wrapper and multivariate regression feature selection techniques were used. The max-flow approach is used by K. Vidhya et al.[12] to obtain optimum segmentation while minimising energy. However, the poor contrast and noise in CT scans make this approach difficult. The authors suggest segmenting lung tumours using the graph cut approach to improve contrast and provide distinct borders. The graph cut approach precisely pinpoints the tumor spot by combining form and area parameters. The approach tries to enhance segmentation outcomes by adding physiological data from the CT image.

3 Methodology

The research flow of LT segmentation and classification of the type of LT is discussed in this chapter. The research flow can be subdivided into three main divisions such as data preparation, segmentation, and classification. The data preparation is the first and essential step to starting the research. In this stage, the data acquisition, process, and augmentation have to be done. The next stage is segmentation, the FCM algorithm is employed to segment the tumor part from the lung CT image. The processing pipeline of segmentation is constructing FCM, training, testing, and evaluation to identify the quality of the model. The final stage is classification; the hybrid approach is utilized for classifying the type of lung tumor from the CT image. The process involved in the pipeline of classification are building the hybrid model and assessment of the model to ensure the quality of the proposed method. In Figure 1, the research flow is depicted.

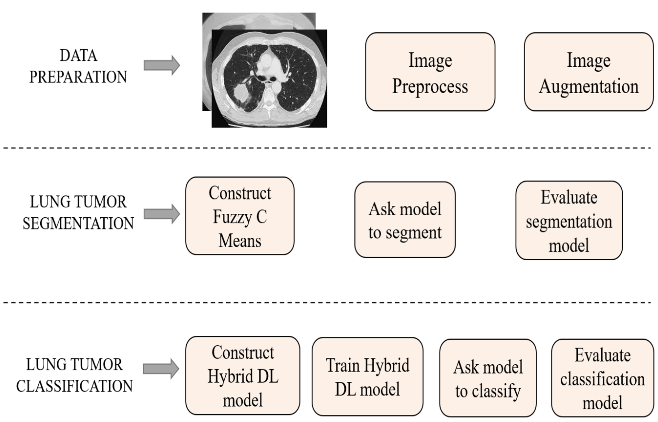

Fig 1. Research flow of DL-based LT segmentation and classification

3.1 Data Preparation

This stage is composed of acquisition, process, and augmentation. In recent times, the development of combined CT imaging has made LT research much easier by making it easier to see where tracer uptake is higher.

3.1.1 Data Collection

A total of 300 individuals from the NSCLC-Radiomics database were employed in this study[13]. For each individual, a digitized three-dimensional area of the chest, including the lungs, heart, and other organs, was made available. DICOM slices of 512 x 512 were produced for all individual instances. Expert radiologists labelled each CT scan with their specialized areas of expertise. The data was split into two groups, one for training (260 individuals) and the other for testing (40 individuals)[13]. The Table 1 displays the total count of axial available slices from each group's CT scan. Figure 2 shows the sample of collected LT images.

Table 1. NSCLC-Radiomics database

Data	Total	Train	Test
Patient Count	300	260	40
Tumor	5144	4296	848
Non-Tumor	30581	26951	3630

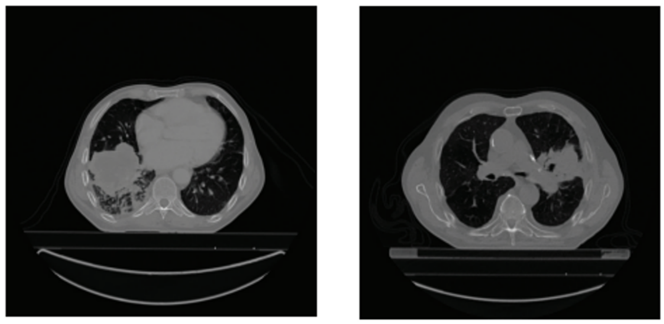

Fig 2. Sample data of LT

3.1.2 Data Preprocess

All images should be reduced to a specific size before being fed into a DL model since NNs only accept inputs of a same size. The collected image should be resized to 256*256. A file with a larger predetermined size is easier to reduce. With less shrinking, the image's details and patterns are less distorted. If this is achieved, distortions would have a lesser effect on classification results. Larger images, on the other hand, not only consume more amount of memory but also lead to a bigger NN. As a result, both the complication of memory and the complication of time increase. It is now evident that selecting a fixed image size involves a trade-off between computing performance and speed. Reducing the boundary pixel or scaling them via interpolation are the two methods for minimizing the dimensionality of images that are larger than the predefined length [14]. Morphology operations refer to image processing procedures that consider shape. To reach the aim of producing an image of a similar size, a structuring element is given to a source image. As a result, while evaluating the pixel in issue, each pixel in the generated image is approximated while taking into consideration the knowledge from the image's neighbouring pixels. This is accomplished by measuring the volume and quality of the area. Morphological techniques are more responsive to certain shapes in an image [15]. The most common and important morphological activities are dilation and erosion. Dilation expands the image by adding pixels, whereas erosion decreases the image size by removing pixels.

Smoothing is indeed an image processing approach to minimize the noise in an image to generate a minimum pixelated and maximum legible image. There are numerous low-pass linear filtering that can be utilized for smoothing. In most circumstances, an average approach or the median static technique is applied. This can enhance the entire appearance of an image. The suggested method employs linear filtration, such as the median filter, being the most common type of filter. When minimizing impulsive noise or salt-and-pepper inside an image, image boundaries and essential characteristics could be kept.

3.1.3 Data Augmentation

The major complaint in DL is a shortage of datasets or a difference in category balancing in databases. One approach to solve this problem is data augmentation [15]. In this work, image recognition relies on a variety of data augmentation approaches, such as translating, rotating, clipping, and magnifying. Figure 3 depicts the output sample of augmented tumor images by horizontal and vertical flipping, and colour variation.

3.2 Tumor Segmentation

To identify abnormal tumor regions in the lungs, physicians use a variety of medical imaging technologies, including CT and MRI. Non-supervised learning approaches, such as FCM and K-Means, are used to segment tumor parts from the CT images. This work employs FCM for the segmentation of LT. To achieve nonlinear data clustering, the FCM combines K-means cluster formation with fuzzy approaches [16]. According to FCM, each image pixel has a membership in the cluster depending on its distance from the cluster's centre, with closer pixels having a greater membership. FCM seeks to minimize the cost function to attain this goal. The FCM technique begins by randomly assigning weights to clusters of values. The center and group

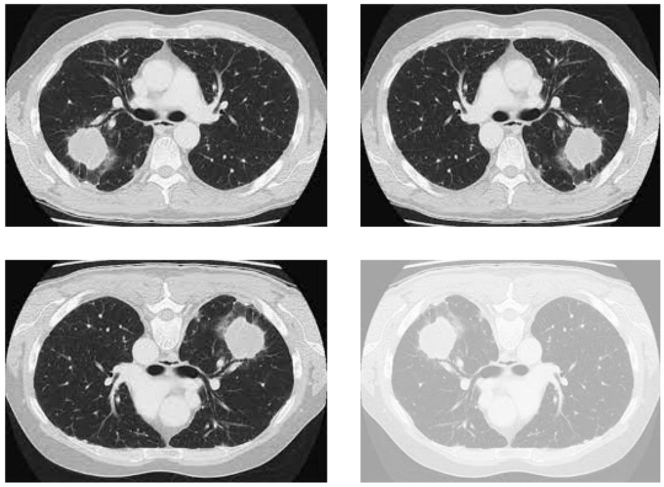

Fig 3. Sample of augmented images

membership weights are then computed repeatedly for every cluster till convergence for every data point is attained.

Fuzzy-based techniques for lung CT image segmentation have lately gained popularity. This technique, unlike hard segmentation techniques, retains significant information from the processed image. Dunn developed the FCM algorithm in 1974, which is based on fuzzy concepts. It has mostly been used in image segmentation ever since. An image pixel may correspond to many classes while employing FCM techniques, and the membership value could vary from zero to one. Hard classification methods, on the other hand, assign a specific category to every pixel. FCM's adaptability led to its application in the segmentation of tumors from CT images. Fast converging and the absence of supervision are some additional advantages of FCM. It is a tough and time-consuming procedure due to the considerable computational time needed by FCM. Furthermore, whenever noise is found, the first estimate choice is delicate, and outlier pixels acquire extremely low membership scores. The concept's most important parameter, C, separates a tumor image of the lungs into several clusters. After the quantity of courses has been established, the estimated centers of every class would be calculated. By providing a membership degree to every data point, centroids will be adjusted continuously to identify the right-center for a set of data. The purpose is to minimize the separation between a data point and the centroid of a cluster by deploying length as an objective function. The membership degree assigned before are used to weight the centroid of all clusters, and a membership function matrix is then generated to assist in the categorization of various parts of an image. The image must be recreated using this membership value matrix. Equation (1) expresses the fundamental objective function of FCM[17].

$$J = \sum_{i=1}^{c} \sum_{p=1}^{n} (u_{ip})^q ||x_p - y_i||^2 \tag{1}$$

Where, u_{ip} denotes a pixel's class p membership value at position i. x_p denotes the image intensity at point p,y_p denotes the class centroid, and c denotes the total classes. The norm in the above equation characterizes the Euclidean distance, whereas the operator q illustrates the weight assigned to each fuzzy membership concerning a specific class. According to the equation, the purpose is to minimize the objective function J by assigning a less membership value to pixels located far from the class's center. In contrast, pixels near the class centroids have more membership scores. The membership parameter u_{ip} and the class centroid y_p are computed using the below equations.

$$u_{ip} = \frac{(||x_p - y_i||)^{-\frac{2}{q-1}}}{\sum_{k=1}^{c} (||x_p - y_k||)^{-\frac{2}{q-1}}} \tag{2}$$

$$y_p = \frac{\sum_{p=1}^{n} (u_{ip})^q x_p}{\sum_{p=1}^{n} (u_{ip})^q} \tag{3}$$

In the equation, $p = 1, \ldots c$ and $c = 1, \ldots n$, where $(||x_p - y_i||)^2$ is frequently used. When the termination criteria are met, the me u_{ip} and y_p *the* function will repeatedly update. The segmented tumor results from the FCM algorithm are shown in Figure 4. The first row contains a raw image of LT, the second row represents the ground truth of the LT image, and finally, the last row consists of FCM segmented output image.

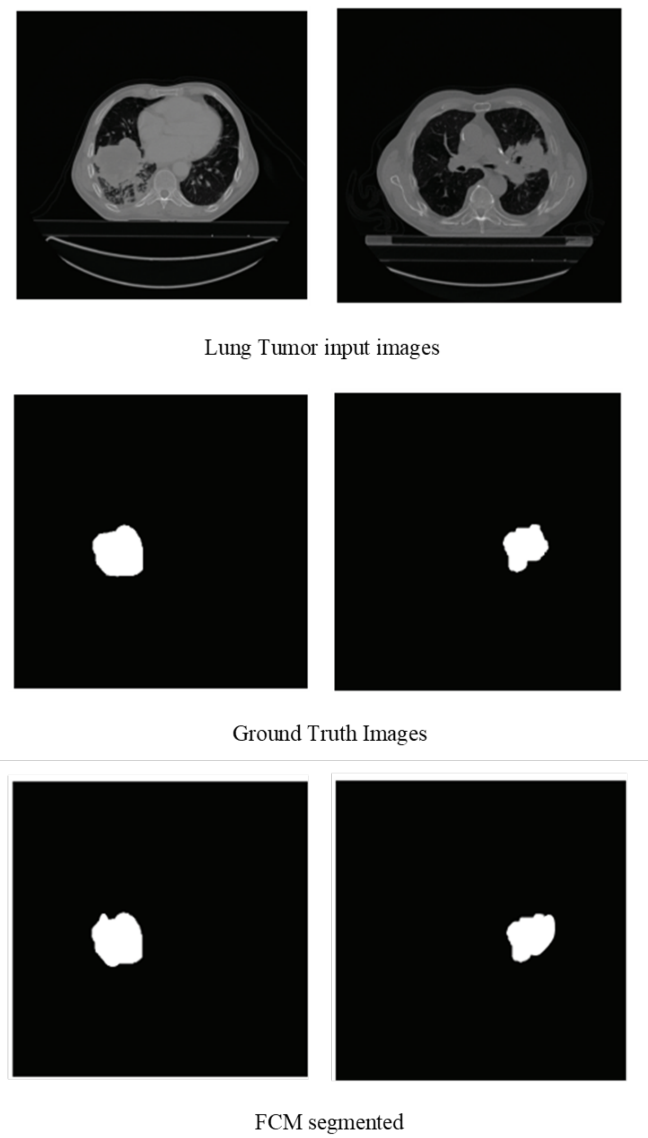

Fig 4. LT segmentation

3.3 Tumor Classification

A CNN is a multi-stage combination of convolutional and fully-connected layers. Convolution techniques are usually used to lower the number of memories needed, and they are executed in a limited area to increase performance. A CNN's four main functions are convolution, non-linear, pool, and fully connected. A CNN is composed of layers, each of which begins with a 2D input sequence, including an image. Every layer contains several kernels. In forward passing processing, it is convolved with each kernel, and dot products are produced between the kernel entries and inputs[18]. A feature map can be created by first performing a linear kernel, then repeatedly implementing a function to various areas of an image, and finally supplying a non-linear function. May obtain the feature map h^k is by using the weights W^k and bias b_k to construct the Kth feature map at a specific layer:

$$h_{ij}^{k} = tanh(W^{k} * x)_{ij} + b_{k} \tag{4}$$

Every hidden layer is made of several feature maps to acquire a more complete image of the input.

$$\left\{h^{k},\ k = 0...K\right\} \tag{5}$$

PCNNs are an evolutionary-inspired method that depends on a cat's visual paradigm. The model is made up of one layer of neurons, each of which is deeply related to a pixel in the input image. A neuron could accept two sorts of inputs: connecting and feeding. The connecting input accepts just local information, whereas the feeding input accepts combined external and internal signals. In this technique, the feeding loop radius of neurons is implemented to determine interior stimuli. The intensity of the matching image pixel, on the other hand, is the source of the external stimuli. The internal perspective of a neuron, which would be the total of its feeding and connecting inputs, determines its output [(19)].

The input images will be labelled with one of the given labels that used a hybrid classification model: "1" - Tumor, and "0" - non-Tumor. The primary objective of PCNNs is to mitigate the influence of poor data-gathering fidelity on the network. While using PCNN image signature creation, no pre-processing or segmentation is required. This signature is employed in feed forward neural layers in conjunction with CNN features. The CNN was tested using various datasets. Each model describes a feature extractor architecture's ability to emphasize a unified feature vector. The combined feature vector is fed into a deep feed forward network to be classified. As a result, CNN's computing load is lowered, and learning data sizes are not limited. There are numerous ways to put this theory into practice, but the PCNN's picture signature creation is a critical component. The first few layers of CNN are frequently employed for tasks like edge detection. Furthermore, the divisions above and below emphasize different components of each class. The hybrid technique can significantly reduce low-quality image resolution and predicted noise [(20)]. Figure 5 depicts the hybrid PCNN and CNN's architecture.

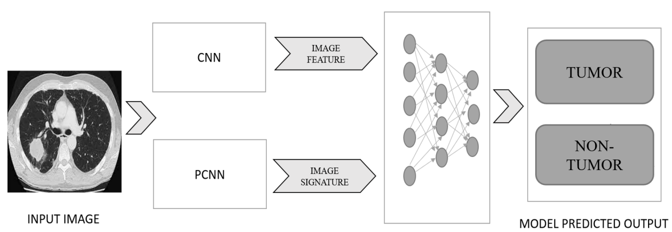

Fig 5. Architecture of PCNN+CNN

4 Results and Discussion

In this section, we evaluate the proposed approach over NSCLC-Radiomics database in terms of Dice similarity, sensitivity, accuracy, Precision, the F1 score, the True Positive Rate (TPR), the True Negative Rate (TNR), the False Positive Rate (FPR), and the False Negative Rate (FNR). The experimental evaluation carried out using python on computer configurations: Intel-i7 with CPU-3.7 GHz, and GPU-Nvidia with memory 11 GB. Section 4.1 described the evaluation metrics, and 4.2 analyzes the performance of proposed approach in comparison with Paing, M. P. et al. [(6)], Fathalla, K. M. et al. [(7)], and Neal Joshua, E. S. et al. [(8)].

4.1 Evaluation Metrics

This subsection describes the evaluation metrics used for analyzing the performance of the proposed approach. Dice similarity and sensitivity are used for evaluating the segmentation performance, whereas TPR and F1 score are used for evaluating the classification performance.

Dice similarity: This metric gauges how similar two sets of data are, and it may be computed using Equation (6).

$$Dice = 2 * \frac{R_p \cap R_a}{R_p + R_a} = \frac{2TP}{2TP + FP + FN} \tag{6}$$

Where R_p and R_a represent the forecast tumor and the actual tumor area in the image.

Accuracy: measures the percentage of pixels in the image which were correctly classified.

$$Accuracy = \frac{TP+TN}{TP+TN+FP+FN} * 100 \tag{7}$$

Where TP denote the correct classification of a tumor, TN denote the correct identification of non-tumor, FP denote the incorrect sorting of a tumor, FN symbolize the wrong identification of non-tumor.

F1 Score: It provides an integrated understanding of the metrics for Precision and Recall. When Precision and Recall are equal, it is at its highest level.

$$F1\ Score = 2\ \times \frac{TP}{TP+FP+FN} * 100 \tag{8}$$

4.2 Performance Analysis

Dice score and sensitivity metrics used to evaluate the segmentation performance of our proposed approach. Our approach accomplished a dice score of 0. 9275. After evaluating the segmentation, the classification process is done. The classification score of our approach compared against the existing approaches shown in Table 2. It depicts the performance evaluation result of the hybrid model.

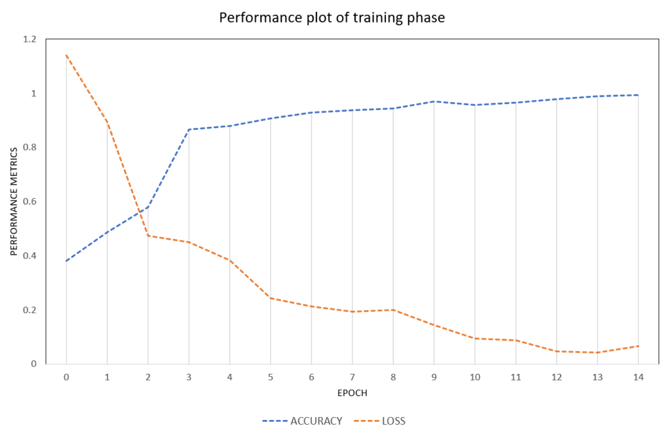

Fig 6. CNN Performance plot

In addition, the suggested hybrid approach is compared with the previous research work done by Neal Joshua et. al, the author used four metrics to validate their model. Those metrics were represented in table and the comparative plots to show the superiority of the suggested model. The proposed approach scores high accuracy and F1-score of 97.43% and of 98.28% respectively, which is better than previous research work as shown in Table 3.

Table 2. Accuracy Comparison

Classification Metric	Ref[7]	Ref[8]	Ref[9]	Proposed
Accuracy	92.8	94	97.17	97.43

Table 3. F1 Score Comparison

Classification Metric	Ref[7]	Ref[8]	Ref[9]	Proposed
F1 Score	92.8	92	92	98.52

5 Conclusion

This research addresses the demanding need for early tumor detection in the context of lung cancer, a leading global cause of mortality. By applying a hybrid deep learning (DL) technique that combines Fuzzy C Means (FCM) for segmentation and a combination of Pulse Coupled Neural Networks (PCNN) and Convolutional Neural Networks (CNN) for classification, the study aims to improve the accuracy and efficiency of tumor detection. The utilization of a hybrid DL approach demonstrates the strengths of FCM, PCNN, and CNN in enhancing tumor identification and classification, offering a potential solution for early diagnosis and treatment planning.

Nevertheless, it is crucial to recognize the constraints of this research. The utilization of web-based data collection introduces potential variability and biases into the dataset, necessitating further validation using larger and more diverse datasets to evaluate generalizability. Furthermore, the scalability and applicability of the proposed approach in real-world clinical settings, coupled with challenges related to computational requirements and interpretability, represent unresolved issues that warrant additional investigation.

Looking ahead, promising prospects and recommendations for future research include refining the hybrid DL approach by leveraging advancements in DL algorithms and incorporating larger annotated datasets. Ongoing developments in medical imaging technologies present opportunities to enhance the proposed method and translate the findings into practical clinical tools. Collaborations between researchers, clinicians, and industry experts can facilitate the integration of the proposed approach into existing healthcare systems, ultimately benefiting patients and healthcare providers by improving lung cancer diagnosis and treatment outcomes.

6 Acknowledgement

The authors extend their sincere gratitude to the Department of PG Studies and Research in Electronics at Kuvempu University for providing the necessary academic support and resources that were crucial to the successful completion of this research.

References

1) Ardila D, Kiraly AP, Bharadwaj S, Choi B, Reicher JJ, Peng L, et al. End-to-end lung cancer screening with three-dimensional deep learning on low-dose chest computed tomography. *Nature Medicine*. 2019;25(6):954–961. Available from: https://doi.org/10.1038/s41591-019-0447-x.
2) Nishio M, Fujimoto K, Matsuo H, Muramatsu C, Sakamoto R, Fujita H. Lung Cancer Segmentation With Transfer Learning: Usefulness of a Pretrained Model Constructed From an Artificial Dataset Generated Using a Generative Adversarial Network. *Frontiers in Artificial Intelligence*. 2021;4:1–10. Available from: https://doi.org/10.3389/frai.2021.694815.
3) Chandrakantha TS, Jagadale BN, Madhuri GR. A Survey on Artificial Intelligence-based Lung Tumor Segmentation and Classification. In: 2022 International Conference on Distributed Computing, VLSI, Electrical Circuits and Robotics (DISCOVER), 14-15 October 2022, Shivamogga, India. IEEE. 2022;p. 201–206. Available from: https://doi.org/10.1109/DISCOVER55800.2022.9974713.
4) Nazir I, Haq IU, Khan MM, Qureshi MB, Ullah H, Butt S. Efficient Pre-Processing and Segmentation for Lung Cancer Detection Using Fused CT Images. *Electronics*. 2022;11(1):1–25. Available from: https://doi.org/10.3390/electronics11010034.
5) Nishio M, Fujimoto K, Matsuo H, Muramatsu C, Sakamoto R, Fujita H. Lung Cancer Segmentation With Transfer Learning: Usefulness of a Pretrained Model Constructed From an Artificial Dataset Generated Using a Generative Adversarial Network. *Frontiers in Artificial Intelligence*. 2021;4:1–10. Available from: https://doi.org/10.3389/frai.2021.694815.
6) Paing MP, Hamamoto K, Tungjitkusolmun S, Pintavirooj C. Automatic Detection and Staging of Lung Tumors using Locational Features and Double-Staged Classifications. *Applied Sciences*. 2019;9(11):1–26. Available from: https://doi.org/10.3390/app9112329.
7) Fathalla KM, Youssef SM, Mohammed N. DETECT-LC: A 3D Deep Learning and Textural Radiomics Computational Model for Lung Cancer Staging and Tumor Phenotyping Based on Computed Tomography Volumes. *Applied Sciences*. 2022;12(13):1–23. Available from: https://doi.org/10.3390/app12136318.
8) Joshua ESN, Bhattacharyya D, Chakkravarthy M, Byun YC. 3D CNN with visual insights for early detection of lung cancer using gradient-weighted class activation. *Journal of Healthcare Engineering*. 2021;2021:1–11. Available from: https://doi.org/10.1155/2021/6695518.
9) Chaunzwa TL, Hosny A, Xu Y, Shafer A, Diao N, Lanuti M, et al. Deep learning classification of lung cancer histology using CT images. *Scientific Reports*. 2021;11(1):1–12. Available from: https://doi.org/10.1038/s41598-021-84630-x.
10) Marentakis P, Karaiskos P, Kouloulias V, Kelekis N, Argentos S, Oikonomopoulos N, et al. Lung cancer histology classification from CT images based on radiomics and deep learning models. *Medical & Biological Engineering & Computing*. 2021;59(1):215–226. Available from: https://doi.org/10.1007/s11517-020-02302-w.
11) Khodabakhshi Z, Mostafaei S, Arabi H, Oveisi M, Shiri I, Zaidi H. Non-small cell lung carcinoma histopathological subtype phenotyping using high-dimensional multinomial multiclass CT radiomics signature. *Computers in Biology and Medicine*. 2021;136:1–9. Available from: https://doi.org/10.1016/j.compbiomed.2021.104752.
12) Vidhya K, Revathi S, Ashwini SSS, Vanitha S. Segmentation of Lung Tumor in CT Images using Graph Cuts. *Indian Journal of Science and Technology*. 2016;9(S1):1–3. Available from: https://doi.org/10.17485/ijst/2016/v9iS1/108428.
13) Zhao B, Kris MG, Schwartz LH. Data From RIDER Lung CT. 2015. Available from: https://doi.org/10.7937/k9/tcia.2015.u1x8a5nr.
14) Hashemi M. Enlarging smaller images before inputting into convolutional neural network: zero-padding vs. interpolation. *Journal of Big Data*. 2019;6(1):1–13. Available from: https://doi.org/10.1186/s40537-019-0263-7.
15) Serra J. Mathematical morphology. In: Sagar BSD, Cheng Q, McKinley J, Agterberg F, editors. Encyclopedia of Mathematical Geosciences. Encyclopedia of Earth Sciences Series;Springer International Publishing. 2022;p. 1–16. Available from: https://doi.org/10.1007/978-3-319-78999-6.
16) Bal A, Banerjee M, Sharma P, Maitra M. Brain Tumor Segmentation on MR Image Using K-Means and Fuzzy-Possibilistic Clustering. In: 2018 2nd International Conference on Electronics, Materials Engineering & Nano-Technology (IEMENTech), 04-05 May 2018, Kolkata, India. IEEE. 2018;p. 1–8. Available from: https://doi.org/10.1109/IEMENTECH.2018.8465390.

17) Pham DL, Prince JL. Adaptive fuzzy segmentation of magnetic resonance images. *IEEE Transactions on Medical Imaging*. 1999;18(9):737–752. Available from: https://doi.org/10.1109/42.802752.
18) Chen L, Li S, Bai Q, Yang J, Jiang S, Miao Y. Review of Image Classification Algorithms Based on Convolutional Neural Networks. *Remote Sensing*. 2021;13(22):1–51. Available from: https://doi.org/10.3390/rs13224712.
19) Shanker R, Bhattacharya M. Classification of brain MR images using Modified version of Simplified Pulse-Coupled Neural Network and Linear Programming Twin Support Vector Machines. *The Journal of Supercomputing*. 2022;78(11):13831–13863. Available from: https://doi.org/10.1007/s11227-022-04420-8.
20) Altaf MM. A hybrid deep learning model for breast cancer diagnosis based on transfer learning and pulse-coupled neural networks. *Mathematical Biosciences and Engineering*. 2021;18(5):5029–5046. Available from: https://doi.org/10.3934/mbe.2021256.